Journal of Molecular Graphics and Modelling 28 (2010) 427–434

Contents lists available at ScienceDirect

Journal of Molecular Graphics and Modelling

journal homepage: www.elsevier.com/locate/JMGM

The modulation of electronic and optical properties of OXD-X through introduction of the electron-withdrawing groups: A DFT study

L.L. Liu, X.M. Pan *, W. Zheng, L.L. Cui, G.C. Yang, Z.M. Su, R.S. Wang

Institute of Functional Material Chemistry, Faculty of Chemistry, Northeast Normal University, Changchun 130024, PR China

ARTICLE INFO

Article history:
Received 26 March 2009
Received in revised form 27 June 2009
Accepted 12 October 2009
Available online 20 October 2009

Keywords:
1,3,4-Oxadiazole compounds
Absorption spectra
Emission spectra
TDDFT
Reorganization energies

ABSTRACT

A comparative study using density functional theory (DFT) on the molecular structure, electronic structure and relative properties of 1,3,4-oxadiazole dimers 1,3-bis[2-(4-methylphenyl)-1,3,4-oxadiazol-5-yl]benzene (OXD-X) and its derivatives with alkoxy substituents $-O(CH_2)_{n-1}CH_3$ (OXD-An, $n = 1$, 2) and electron-withdrawing substituents –CN (OXD-C), $-CF_3$ (OXD-TFM), $-NO_2$ (OXD-N) added at meta-substitution in the phenyl ring are presented. The ground state structures of the title complexes are optimized at B3LYP/6-31G level of theory. In addition, the time dependent density functional theory (TDDFT) method is applied to calculate the absorption and emission spectra of the derivatives based on the ground state geometries. Comparing with the alkoxy substituents, the results show that the electron-withdrawing substituents have remarkable influences on the energy levels of the frontier molecular orbitals, the spectra and the transition compositions. Especially, $-NO_2$ group plays the prominent role and the fluorine improves the energy level of LUMO further. The experimental absorption wavelengths for OXD-X, OXD-A3 and OXD-A7 are well reproduced by the TDDFT technique. Moreover the absorption wavelengths and the transition compositions can be effectively adjusted through introducing electro-withdrawing groups in the phenyl ring. The reorganization energies for hole and electron are smaller than that of typical hole and electron transport materials.

1. Introduction

Recently organic light-emitting diodes (OLEDs) have attracted a great deal of attention after the reports by Tang and Van Slyke et al. in 1987 due to their promising applications in electroluminescent displays [1]. One of the most important goals of research on organic materials for electroluminescent displays is the preparation of good electron-accepting and -transporting (n-type) materials [2–4]. Most organic materials are p-type materials, and the ability of accepting and transporting holes is better than that of electrons, but n-type materials are urgently needed in n-type transistors as a result of the abilities of electron injection and transport [5]. In previous years, a large number of organic compounds were prepared for the purpose of fabricating efficient electron-accepting and -transporting materials, among which molecular and polymeric 1,3,4-oxadiazole (OXD) derivatives have afforded several appealing advantages over other materials [6–9]. The experimental investigation shows that introducing an electron-deficient oxadiazole group will result in increasing electron affinity of the compound, which facilitates electron injection and transport as well as the balanced charge recombination in the emissive layer [10,11]. Recently, many quantum chemical techniques, such as density functional theory (DFT), time dependent DFT (TDDFT), ab initio and semiempirical levels are successfully applied to investigating the geometry structures, electronic and optical properties of 1,3,4-oxadiazole derivatives [12,13]. The theoretical results show that the strong push–pull effect of oxadiazole ring on electron density may be affected by the weak interaction between the nitrogen and oxygen atoms. In addition, introducing oxadiazole not only decreases the HOMO and LUMO energy level but also enhances the electron conjugation over the whole molecule and thus stabilizes the LUMOs.

In the previous work, Tian et al. has succeeded in preparing a series of 1,3,4-oxadiazole dimmers (OXD-X) and its derivatives, which are substituted with different alkoxy groups ($-O(CH_2)_{n-1}CH_3$, $-O(CH_2)_nOC_6H_5CH_3$, $-O(CH_2)_nOC_6H_4NNC_6H_4OCH_3$) in the side chain [14]. The result shows that the alkoxy substituents affect the electron-donating and accepting abilities of the species. Especially, the substituent $-O(CH_2)_nOC_6H_4NNC_6H_4OCH_3$ enhances the electron injection ability.

Karasz et al. reported that the compounds are modified by –CN, $-CF_3$ and $-NO_2$, and exhibit good charge injection and transport properties [15–17]. The electron-withdrawing groups are responsible for the high electron affinity, which is a desirable property

* Corresponding author. Tel.: +86 431 85099963; fax: +86 431 85099511.
E-mail address: panxm460@nenu.edu.cn (X.M. Pan).

1093-3263/$ – see front matter © 2009 Elsevier Inc. All rights reserved.
doi:10.1016/j.jmgm.2009.10.002

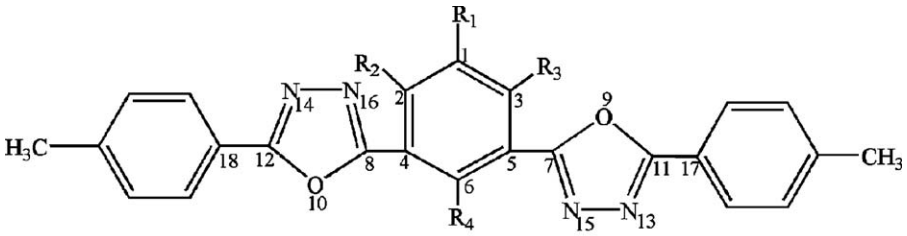

Derivatives	R_1	R_2	R_3	R_4
OXD-X	H			
OXD-A3	$-O(CH_2)_2CH_3$			
OXD-A7	$-O(CH_2)_6CH_3$			
OXD-TFM	$-CF_3$			
OXD-C	-CN			
OXD-N	$-NO_2$			
OXD-N-1	$-NO_2$	H	H	F
OXD-N-2	$-NO_2$	H	F	F
OXD-N-3	$-NO_2$	F	F	F

Fig. 1. Molecular structures of the 1,3,4-oxadiazole derivatives.

because the stable metal electrodes, such as aluminum, can be used for electron injection. In addition, –CN and $–NO_2$ have a large influence on the lowest unoccupied molecular orbital (LUMO) through π orbital interactions and result in the red shift of absorption wavelengths with respect to the electron-donating group [18–20]. In this paper, we use a serious of electron-withdrawing groups ($–CF_3$, –CN, $–NO_2$) in the side chain of the OXD-X as meta-substitution, and settle F on the central phenyl ring as ortho-substitution. For the new serious of OXD-X derivatives, the energy levels of the frontier molecular orbitals exhibit dramatic variation after adding electron-withdrawing groups. In addition, the ionization potential (IP) and the electron affinity (EA) as well as the absorption and emission spectra of the new derivatives change obviously. We hope that our theoretical investigation on the IP, EA, and band gaps of the compounds is helpful to the experimental synthesis. Therefore, we perform a density functional theory (DFT) study on the structures, absorption and emission spectra of nine OXD-X derivatives, and explore the effect of electron-withdrawing groups on the electronic and optical properties.

2. Computation details

All the calculations are performed by Gaussian 03 program suite [21]. The B3LYP functional, involving the gradient correction of the exchange functional by Becke [22,23] and the correction functional by Lee, Yang and Parr [24], and 6-31G basis set are employed. The ground state calculation of OXD-X is also performed by B3LYP with 6-31G* and 6-31G** basis sets, respectively. It is found that the main bond lengths of the OXD-X obtained by B3LYP/6-31G* and B3LYP/6-31G** calculations are nearly equal to that obtained by B3LYP/6-31G. The time dependent density functional theory (TDDFT) approach [25] with the same basis sets is applied to investigate the properties of spectra and electronic transition mechanism which are based on the ground state geometry of OXD-X. Meanwhile, comparing with that under B3LYP/6-31G, the calculated maximal absorption wavelengths under B3LYP/6-31G* and B3LYP/6-31G** have no obvious difference. So, we use the 6-31G basis set for our calculations. The lowest singlet excited states are computed with ab initio CIS/6-31G on the basis of the optimized geometries, which are obtained from HF/6-31G calculations. The emission spectra are predicted by time dependent TDDFT with 6-31G basis set. In addition, the π-conjugated compounds have a more important feature after oxidative (p-type) or reductive (n-type) doping. So, the cationic and anionic systems of nine derivatives are also optimized at B3LYP/6-31G levels.

3. Results and discussion

3.1. Ground state geometry

The sketch of the structures for OXD-X, OXD-A3, OXD-A7, OXD-TFM, OXD-C, OXD-N, OXD-N-1, OXD-N-2 and OXD-N-3 is depicted in Fig. 1. Tian et al. theoretically reported the ground state structures of OXD-X and OXD-A3 only in cis-conformation. In the paper, in order to determine the minimum energy configuration as well as energy difference between the cis- and trans-conformation, we perform geometrical optimizations on the 1,3,4-oxadiazole derivatives fully. The relative energies of the trans- and cis-conformations for the 1,3,4-oxadiazole derivatives obtained by B3LYP/6-31G calculations are shown in Table 1. The results show that the trans-conformation is more stable than the cis-one. For example, the energies of trans-OXD-N is lower by 4.06 kJ/mol than the cis-one. As to the OXD-N substituted with fluorine atoms, the energy differences increase with the increase of fluorine atoms, due to the strong push–pull effect between the fluorine atoms and the central benzene ring. So the trans-conformations are chosen in this paper. From the theoretical point of view, there are three stable isomers for the OXD-N substituted by singlet fluorine. The relative energy of the isomer with fluorine substituted at C_6 is 4.77 kJ/mol and is smaller by 3.77 kJ/mol than that of substituted at C_2 and C_3. We name the geometry with fluorine atom substituted at C_6 as OXD-N-1. From Fig. 1, it can be found that, the position of double fluorines substituted OXD-N can locate on C_2, C_3, C_2, C_6, or C_3, C_6. The relative energy which C_3, C_6 substituted is 1.57 kJ/mol and smaller by 0.94 kJ/mol than that substituted at C_2, C_3 or C_2, C_6. Thus, the isomer with double fluorines substituted at C_3, C_6 is named OXD-N-2.

In order to investigate the substituent effect on the OXD derivatives, the electron-donating substituents (OXD-A3 and -A7), and the electron-withdrawing substituents (OXD-TFM, -C, -N) are added with meta-substitution in the phenyl ring of OXD (Fig. 1). The meta-substituted OXD derivatives are nearly planar conformations, indicating that introducing alkoxy chains, $–CF_3$, –CN and $–NO_2$ on the central benzene ring have little effect on the π-conjugated backbone of the whole molecular. As for the OXD derivatives, the main bond lengths have no obvious change.

Table 1
The relative energies ΔE (kJ/mole) of the trans- and cis-conformations for the 1,3,4-oxadiazole derivatives obtained by B3LYP/6-31G calculations.

Compounds	OXD-X	OXD-A3	OXD-A7	OXD-TFM	OXD-C	OXD-N	OXD-N-1	OXD-N-2	OXD-N-3
ΔE	−0.33	−1.84	−1.67	−2.64	−2.34	−4.06	−1.09	−3.39	−20.59

However, for the OXD-N-3 with ortho-substitution (Fig. 2), the dihedral angle between 1,3,4-oxadiazole ring and the central benzene ring is 30°. In addition, there is a large torsion between $-NO_2$ and the central benzene ring. The result suggests that introducing three fluorine atoms on the central benzene ring creates much more steric hindrance than introducing one or two fluorine atoms. And the structural character of OXD-N-3 blocks the conjugation of backbone between the neighborhood fragments. According to the analysis of geometric structures of OXD derivatives, the meta-substitution in the phenyl ring of OXDs generates less steric effect than that of ortho-substitutions.

3.2. Frontier molecular orbitals

The frontier molecular orbitals (FMOs) of the 1,3,4-oxadiazole derivatives are shown in Fig. 3. Fig. 4 lists the energies of the frontier molecular orbitals for nine derivatives. It will be useful to examine the highest occupied orbitals (HOMOs) and the lowest virtual orbitals (LUMOs) for these derivatives because the relative ordering of the occupied and virtual orbitals provide a reasonable qualitative indication of the excitation properties and of the ability of electron or hole transport.

As to the electron-donation substituted OXDs, the LUMO distributions of OXD-A3 and OXD-A7 are similar to that of OXD-X located on the right part of the molecular backbone, but the HOMOs mainly localized on the left part which are different from that of OXD-X separated over the whole molecule. In addition, when an alkoxy group as meta-substitution, the 2p(O) orbital ($-O(CH_2)_2CH_3$) participates in the composition of HOMO. As above saying, all molecules are trans-conformations. Tian et al. reported the electronic structures of cis-OXD-X and OXD-A3 and discovered that the LUMO distribution of OXD-A3 is similar to that of OXD-X, and the HOMO is slightly different from that of OXD-X [14]. As to the energy level, the HOMO and LUMO values for OXD-A3 and OXD-A7 are −6.23 and −1.98 eV, −6.22 and −1.97 eV, respectively. And comparing with OXD-X (−6.28, −2.03 eV) (Fig. 4), the values increase ~0.05 eV. The results suggest that introducing electron-donating groups ($-O(CH_2)_2CH_3$ and $-O(CH_2)_6CH_3$) increases the π electron density of the central benzene ring and thus the values of HOMO and LUMO increase.

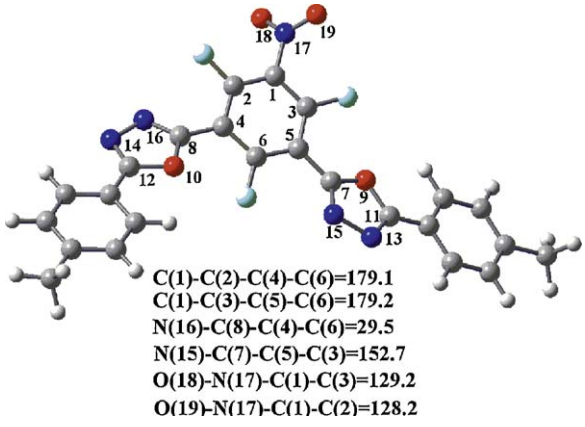

Fig. 2. Optimized structures and main dihedral angles (degrees) of OXD-N-3.

In contrast, comparing with the corresponding electron-donating groups, the introduction of electron-withdrawing groups ($-CF_3$, $-CN$, $-NO_2$) results in a large decrease on the energy levels of the main FMOs. Because the electron-withdrawing groups reduce the π-electron density of the central phenyl ring and thus the energies of HOMO and LUMO decrease [15]. As shown in Fig. 3, the HOMO distributions for electron-donation substituted OXDs are similar to that of OXD-X, but the LUMO mainly localized on the central phenyl ring and substitution, especially for the compounds substituted by $-NO_2$. From Fig. 4, it can be seen that the energy levels of LUMO decrease by 0.37 and 0.40 eV from OXD-X (−2.03 eV) to OXD-TFM (−2.40 eV) and OXD-C (−2.43 eV). Especially, comparing with that of OXD-X, the LUMO of OXD-N (−3.22 eV) is much more stabilized about 1.19 eV, and is lower by 1.12 eV than that of OXD-C3(2.10 eV) calculated by Tian et al. [14]. It indicates that the electron-accepting ability is improved by the introduction of the electron-withdrawing group $-NO_2$. The reason can be explained that, from the density diagram plots of the FMOs (Fig. 3), it can be found that the LUMO of OXD-N is mostly localized on $-NO_2$ and the central benzene ring, which the composition mainly comes from p_z orbital of N, O and C. The strong localization effect of the electronic cloud can be attributed to the mixed electron withdrawing and conjugation effect of $-NO_2$ group, which is related to the large decrease of the LUMO energy. As to the evolution of the HOMO levels, comparing with OXD-X (−6.28 eV), the energies of OXD-TFM (−6.53 eV), OXD-C (−6.56 eV) and OXD-N (−6.62 eV) are generally stabilized about 0.25, 0.28 and 0.34 eV. As a result, the energy gaps decrease, $4.25 < 4.13 = 4.13 < 3.40$ eV, going from OXD-X to OXD-TFM, to OXD-C, and to OXD-N. The above results suggest that adding the electron-withdrawing groups to meta-substitution can effectively stabilize the energy of the FMOs. The electron-accepting properties and the energy gaps of the derivatives are greatly adjusted by the introduction of $-CF_3$, $-CN$, $-NO_2$ groups. Especially, comparing with the other electron-withdrawing groups, $-NO_2$ group plays the prominent role of modulating the FMO levels and the energy gaps of the derivatives.

Park reports that the substitution of fluorine can make the energies of HOMO and LUMO decrease because of the property of the fluorine atom withdrawing electrons. Especially, the withdrawing affects the radical where it is suspended [26]. So, if the atom is bound to molecular segment of the radical functioning LUMO, the decreasing tendency of the energy level of LUMO is more significant than that of HOMO. Additionally, one of the most important features of the π-conjugated polymers is their ability to become highly conducted after oxidative (p-type) or reductive (n-type) doping. Fluorine atom as electron acceptor can be used as reductive (n-type) doping. So, in order to further decrease the energy levels of LUMO, from these viewpoints, it would be thought that the fluorine atom is located on the central phenyl part with $-NO_2$ which plays the role of LUMO. As is expected, comparing with the energy of LUMO of OXD-N (Fig. 4), OXD-N-1 decreases by 0.09 eV, OXD-N-2 decreases 0.06 eV, and OXD-N-3 decreases 0.19 eV. It indicates that introducing fluorine can further decrease the LUMO energy, which is benefit for improving the electron-accepting abilities of OXD-N.

3.3. Absorption spectra

The absorption spectra for OXD-X obtained by B3LYP/6-31G* and B3LYP/6-31G** are identical with B3LYP/6-31G. So, B3LYP/6-31G is

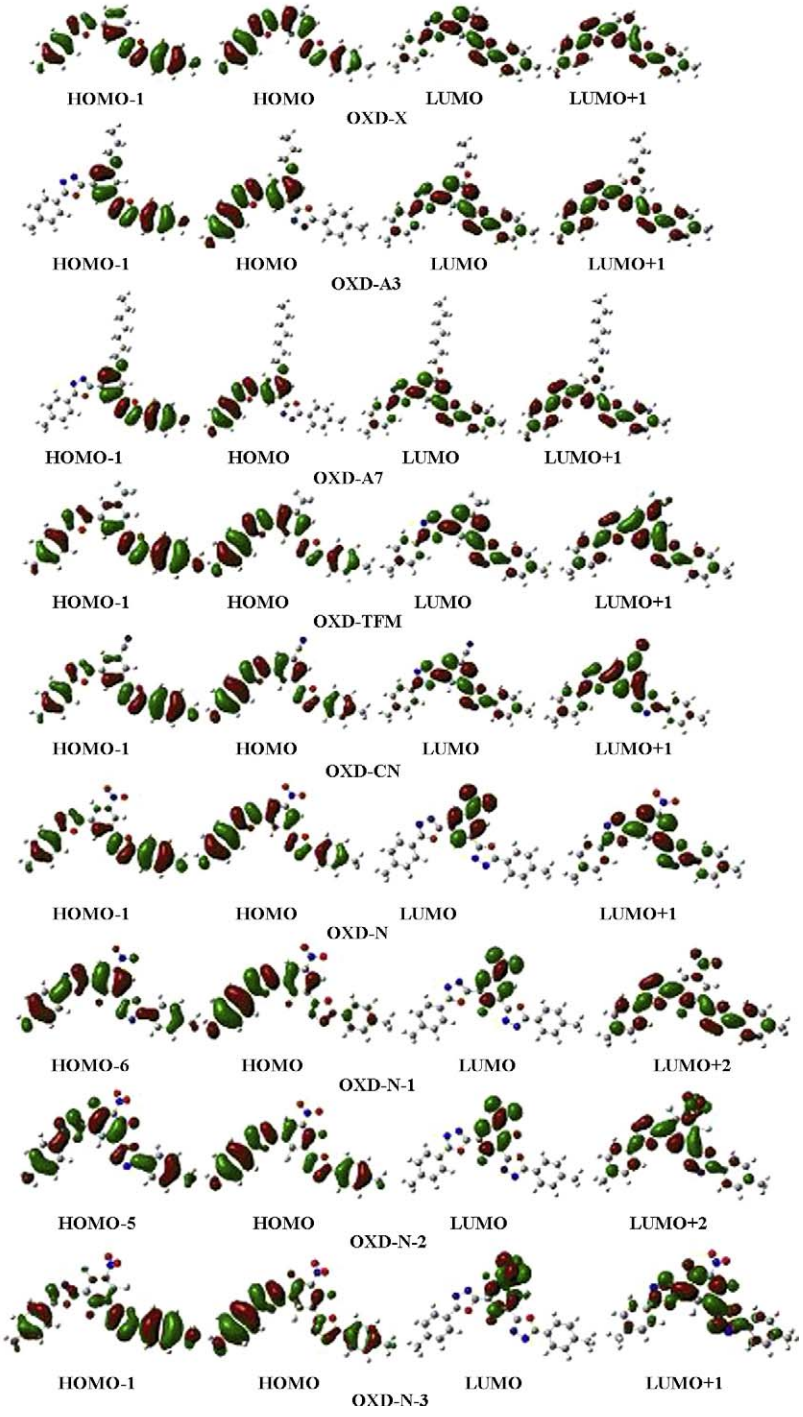

Fig. 3. The frontier molecular orbitals (FMOs) for the 1,3,4-oxadiazole derivatives in the ground states.

chosen to calculate absorption spectra. Electronic absorption transition data obtained by the TDDFT//B3LYP/6-31G for the 1,3,4-oxadiazole derivatives are listed in Table 2. The calculated absorption wavelengths for OXD-X, OXD-A3 and OXD-A7 are 312, 306 and 306 nm, respectively, which are in good agreement with the experimental results [14]. For OXD-X, the strongest absorption peak is assigned to $\pi \rightarrow \pi^*$ electronic transition character arising from $S_0 \rightarrow S_2$ electronic transition which is composed by HOMO -→ LUMO (32%), HOMO → LUMO+1 (30%) and HOMO−1 → LUMO (28%). As to alkoxy substituent derivatives, the main absorption peaks are mostly composed by HOMO → LUMO+1 (53% for OXD-A3 and 52% for OXD-A7) that arises from $S_0 \rightarrow S_3$ electronic transition. The results suggest that the alkoxy group mainly changes the compositions of the transition. The absorption wavelengths of the derivatives change little through increasing the length of the flexible chain.

As to electron-donation substituted OXDs, the main excitations also correspond to the promotion of an electron from HOMO -→ LUMO+1 for OXD-TFM and OXD-C. However, comparing with that of the alkoxy substituted derivatives (53%, 52%), the transition percentages (79%, 70%) are greatly improved. The absorption wavelengths for OXD-TFM and OXD-C are 317.9 and 324.6 nm. In addition, the transition energies (3.90, 3.82 eV) are slightly smaller than those of the alkoxy substituted derivatives (4.05 eV), which

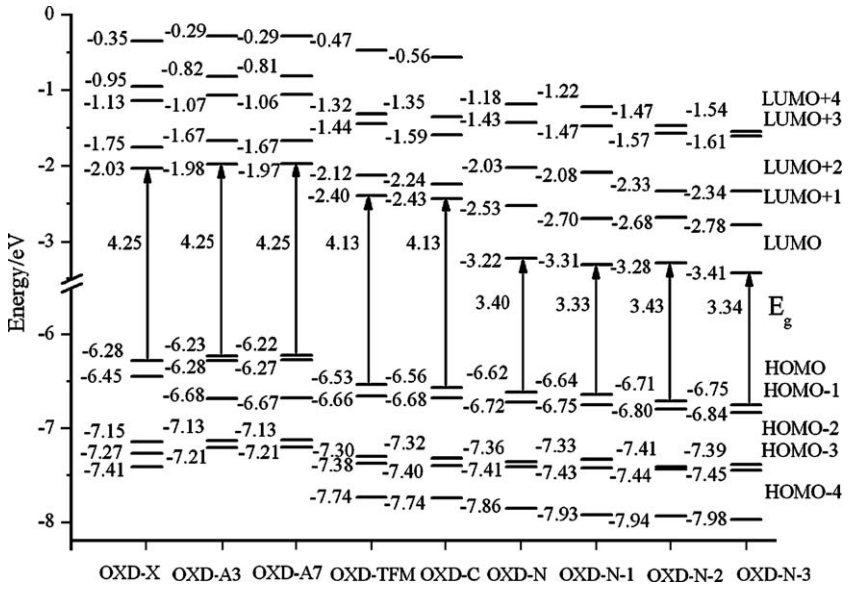

Fig. 4. Diagrams of energies of the frontier molecular orbitals in the 1,3,4-oxadiazole derivatives.

finally results in the red shift of the wavelengths for ~27 and ~34 nm, respectively. For OXD-N, the absorption wavelength is 335.1 nm, introducing $-NO_2$ leads to a red shift compared to that of the $-CF_3$ and –CN substituted derivatives (Table 2). The main excitation is changed to HOMO−1 → LUMO+1 (66%). The strongest absorption peaks of OXD-N-1, OXD-N-2 and OXD-N-3 are mostly composed by HOMO → LUMO+2 (66%), HOMO → LUMO+2 (88%) and HOMO−1 → LUMO+1 (61%) of $S_0 \rightarrow S_9$, $S_0 \rightarrow S_{10}$ and $S_0 \rightarrow S_4$ transition, and the absorption wavelength shows to the red shift, $302 < 307 < 348$ nm, resulting from excitation energies decreasing, $4.10 > 4.04 > 3.57$ eV. The result suggests that the absorption wavelengths can be effectively adjusted through introducing different electron-withdrawing substituents. In addition, the absorption spectra of $-NO_2$ substituted derivatives can be further modulated through changing the position or the quantity of fluorine.

3.4. Properties of excited structures and emission spectra

Up to now, the standard for optimization of excited-state equilibrium properties of larger molecules in the Gaussian program package is the configuration interaction singles (CIS) method. However, due to the neglect of electron correlation, CIS results are not accurate enough in many applications. We optimize the title compounds by CIS/6-31G and compare with their ground structures by HF/6-31G. The compared results of main bond lengths between the excited and ground states are shown in Table 3.

Table 2
Electronic absorption transition data obtained by the TDDFT//B3LYP/6-31G for the 1,3,4-oxadiazole derivatives.

Compounds	Electronic transition	Composition		f	ΔE (eV)/λ(nm)	Exp.[a]
OXD-X	$S_0 \rightarrow S_2$	HOMO → LUMO	32%	0.9150	3.98/311.6	292
		HOMO → LUMO+1	30%			
		HOMO−1 → LUMO	28%			
OXD-A3	$S_0 \rightarrow S_3$	HOMO → LUMO+1	53%	1.0217	4.05/306.1	291
		HOMO−1 → LUMO+1	23%			
		HOMO−2 → LUMO	12%			
OXD-A7	$S_0 \rightarrow S_3$	HOMO → LUMO+1	52%	1.0257	4.05/306.1	291
		HOMO−1 → LUMO+1	24%			
		HOMO−2 → LUMO	12%			
OXD-TFM	$S_0 \rightarrow S_3$	HOMO → LUMO+1	79%	0.5377	3.90/317.9	
		HOMO → LUMO	7%			
OXD-C	$S_0 \rightarrow S_2$	HOMO → LUMO+1	70%	0.9332	3.82/324.6	
		HOMO−1 → LUMO	19%			
OXD-N	$S_0 \rightarrow S_4$	HOMO−1 → LUMO+1	66%	0.5672	3.70/335.1	
		HOMO → LUMO+1	27%			
OXD-N-1	$S_0 \rightarrow S_9$	HOMO → LUMO+2	66%	0.5709	4.10/302.1	
		HOMO−6 → LUMO	17%			
		HOMO−1 → LUMO+2	6%			
OXD-N-2	$S_0 \rightarrow S_{10}$	HOMO → LUMO+2	82%	0.5906	4.04/306.6	
		HOMO−5 → LUMO	8%			
OXD-N-3	$S_0 \rightarrow S_4$	HOMO−1 → LUMO+1	61%	0.4683	3.57/347.8	
		HOMO → LUMO+1	34%			

[a] The experiment data are given from Ref. [14].

Table 3
Selected bond lengths (nm) of the 1,3,4-oxadiazole derivatives in the ground states with HF/6-31G and excited states with CIS/6-31G.

Parameters		OXD-X	OXD-A3	OXD-A7	OXD-TFM	OXD-C	OCD-N
r(4,8)	HF	0.1453	0.1454	0.1454	0.1453	0.1453	0.1452
	CIS	0.1397	0.1454	0.1454	0.1454	0.1457	0.1403
r(5,7)	HF	0.1453	0.1454	0.1454	0.1453	0.1453	0.1452
	CIS	0.1454	0.1396	0.1396	0.1396	0.1402	0.1468
r(18,12)	HF	0.1451	0.1451	0.1452	0.1451	0.1451	0.1450
	CIS	0.1393	0.1451	0.1451	0.1450	0.1464	0.1400
r(11,17)	HF	0.1451	0.1451	0.1451	0.1451	0.1451	0.1450
	CIS	0.1451	0.1395	0.1395	0.1393	0.1401	0.1463

Table 4
Electronic emission spectra transition data obtained by the TDDFT//B3LYP/6-31G for the 1,3,4-oxadiazole derivatives.

Compounds	Electronic transition	Composition		*f*	Δ*E* (eV)/λ (nm)
OXD-X	$S_1 \rightarrow S_0$	HOMO → LUMO	79%	1.1791	3.52/352.2
OXD-A3	$S_1 \rightarrow S_0$	HOMO → LUMO	75%	1.0034	3.43/361.2
		HOMO−1 → LUMO	6%		
OXD-A7	$S_1 \rightarrow S_0$	HOMO → LUMO	75%	0.9922	3.43/361.4
		HOMO−1 → LUMO	6%		
OXD-TFM	$S_1 \rightarrow S_0$	HOMO → LUMO	79%	1.1140	3.45/359.6
OXD-C	$S_1 \rightarrow S_0$	HOMO → LUMO	80%	1.0972	3.52/351.8
OXD-N	$S_2 \rightarrow S_0$	HOMO−1 → LUMO+1	68%	0.7805	3.51/353.6
		HOMO → LUMO	8%		
		HOMO−1 → LUMO	6%		
OXD-N-1	$S_2 \rightarrow S_0$	HOMO → LUMO+1	57%	0.7821	3.37/367.7
		HOMO → LUMO	22%		
OXD-N-2	$S_6 \rightarrow S_0$	HOMO−1 → LUMO+1	70%	0.4690	4.04/306.6
		HOMO → LUMO+1	25%		
OXD-N-3	$S_9 \rightarrow S_0$	HOMO−1 → LUMO+1	68%	0.4279	3.67/337.6
		HOMO → LUMO+1	26%		

As shown, most selected bonds obtained by CIS give shorter than that obtained by HF method. In fact, we can predict the differences in the bond lengths between the ground (S_0) and single excited state (S_1) from MO nodal patterns. We explore the bond length variations by analyzing the HOMO and LUMO. By comparison of Table 3 with Fig. 3, the HOMO is antibonding across *r*(4,8), *r*(5,7), *r*(18,12), *r*(11,17) bonds in all compounds, but the LUMO is bonding in these regions. Hence, removing an electron from HOMO leads to the shortening of the bond distances in the excited state. Therefore, one would expect contraction of these bonds; the data in Table 3 show that these bonds are in fact considerably shorter in the excited state. For instance, the bond *r*(4,8) is 0.1397 nm by CIS method in the excited state, which is shorter than that (0.1453 nm) by HF method in the ground state.

Consequently, the emission spectra calculations are made on the basis of the optimized geometries by CIS method, using the TD calculations employing the B3LYP/6-31G method from the singlet ground state to the ten singlet excited states, and the data are listed in Table 4. Similar to absorption spectra, the emission spectra of OXD-A3 is identical with OXD-A7, indicating that the length of alkoxy have little effect on emission spectra. The emission peaks with strongest oscillator strength are all assigned to $\pi \rightarrow \pi^*$ character arising from S_1, HOMO to LUMO transition. The emission spectra of OXD-TFM, OXD-C, OXD-N are 359.6, 351.8, 353.6 nm, exhibiting blue shift compared with electron-donation substituted OXDs. The emission spectra of difluorine and trifluorine substituted compounds, which exhibits a blue shift compared with that of the compounds substituted by one fluorine atom, 367.7 > 306.6 nm, going from OXD-N-1 to OXD-N-2, and 367.7 > 337.6 nm, going from OXD-N-1 to OXD-N-3.

3.5. Ionic states properties

3.5.1. The optimized geometries in ionic states

The cationic and anionic geometries of 1,3,4-oxadiazole derivatives are optimized by B3LYP/6-31G, and selected important bond lengths are compiled in Table 5. Comparing with that of neutral states, the dihedral angles are nearly 0.0° and the important bond lengths are shorter in cationic and anionic states of OXD-X, OXD-A3, OXD-A7, OXD-TFM and OXD-C, which indicates that the π-conjugation backbone is well maintained. It can also be analysed from FMOs. On the one hand, there are antibonding

Table 5
Selected bond lengths (nm) of the 1,3,4-oxadiazole derivatives in the neutral, cationic and anionic states obtained by B3LYP/6-31G calculations.

Parameters	OXD-X	OXD-A3	OXD-A7	OXD-TFM	OXD-C	OXD-N
Neutral state						
r(4,8)	0.1451	0.1451	0.1451	0.1451	0.1451	0.1408
r(5,7)	0.1451	0.1451	0.1451	0.1451	0.1451	0.1407
r(18,12)	0.1448	0.1448	0.1448	0.1447	0.1447	0.1447
r(11,17)	0.1448	0.1448	0.1448	0.1447	0.1447	0.1447
Cationic state						
r(4,8)	0.1436	0.1435	0.1435	0.1438	0.1439	0.1440
r(5,7)	0.1437	0.1438	0.1438	0.1439	0.1440	0.1440
r(18,12)	0.1427	0.1427	0.1427	0.1427	0.1427	0.1427
r(11,17)	0.1429	0.1430	0.1430	0.1429	0.1429	0.1429
Anionic state						
r(4,8)	0.1433	0.1431	0.1431	0.1429	0.1430	0.1446
r(5,7)	0.1433	0.1433	0.1433	0.1430	0.1430	0.1445
r(18,12)	0.1439	0.1439	0.1439	0.1441	0.1442	0.1447
r(11,17)	0.1435	0.1436	0.1436	0.1439	0.1439	0.1449

Table 6
Ionization potentials, electron affinities, extraction potentials and reorganization energies (eV) for each derivative Calculated by DFT//B3LYP/6-31G[a].

Compounds	IP(v)	IP(a)	HEP	EA(v)	EA(a)	EEP	λ(h)	λ(e)
OXD-X	7.45	7.34	7.24	0.79	0.87	0.96	0.21	0.17
OXD-A3	7.39	7.28	7.18	0.77	0.87	0.97	0.21	0.20
OXD-A7	7.38	7.27	7.16	0.77	0.87	0.97	0.22	0.20
OXD-TFM	7.68	7.59	7.49	1.13	1.24	1.34	0.19	0.21
OXD-C	7.70	7.61	7.52	1.18	1.28	1.37	0.18	0.19
OXD-N	7.76	7.67	7.57	1.49	1.68	1.87	0.19	0.38
OXD-N-1	7.79	7.70	7.61	1.58	1.76	1.96	0.18	0.38
OXD-N-2	7.81	7.72	7.63	1.69	1.87	2.05	0.18	0.36
OXD-N-3	7.90	7.78	7.68	1.63	1.86	2.10	0.22	0.47

[a] The suffixes (v) and (a) indicate vertical and adiabatic values, respectively.

orbitals among the neighborhood subunits, hence, comparing with the neutral state, removing an electron from HOMO leads to a shortening of the antibonding distances in cationic state. On the other hand, the LUMOs of five derivatives generally show a bonding character among the neighborhood subunits. So, comparing with the neutral state, immigrating an electron from LUMO leads to shorten in anionic state. The shortening of the distances mentioned above is due to the bonding interactions among the π orbitals on the two adjacent subunits. For the $-NO_2$ substituted derivatives, comparing with the neutral state, the changes of the bond lengths in anionic state are mainly focus on the bond between central benzene ring and $-NO_2$, which suggests that the electron injection position is mainly located on the central benzene ring and $-NO_2$. The result is consistent with the distribution of the LUMOs for these derivatives.

3.5.2. Ionization potentials and electron affinities

The adequate and balanced transport of both injected electrons and holes are important in optimizing the performance of OLED devices. The ionization potential (IP) and electron affinity (EA) are well-defined properties that can be calculated by DFT on the geometries in the neutral, cationic and anionic sates and estimated the energy barrier for the injection of both holes and electrons into the derivatives. Table 6 contains the IPs, EAs, both vertical (v: at the geometry of the neutral molecule) and adiabatic excitations (a: optimized structure for both the neutral and charged molecule) and the extraction potentials (HEP and EEP for the hole and electron, respectively) that refer to the geometry of the ions.

For OXD-TFM, OXD-C and OXD-N, the energy required to create a hole in the derivatives is 7.68, 7.70 and 7.76 eV, respectively, which is higher than that in OXD-X (7.45 eV), suggesting that it is difficult to create a hole in electro-withdrawing substituted derivatives than in OXD-X and the hole blocking ability is efficiently improved by the introduction of $-CF_3$, –CN and $-NO_2$. In addition, the extraction of an electron from the anion requires 1.13, 1.18 and 1.49 eV for OXD-TFM, OXD-C and OXD-N, which are largely higher than the corresponding OXD-X (0.79 eV) by 0.34, 0.39 and 0.70 eV. This indicates that the electron-accepting and -transporting properties have been greatly improved in OXD-TFM, OXD-C and OXD-N. Especially, introducing $-NO_2$ can effectively enhanced the EAs. In the mean while, the EAs are further adjusted through introducing fluorine in OXD-N, which are 1.58 eV (OXD-N-1), 1.69 eV (OXD-N-2) and 1.63 eV (OXD-N-3), respectively. The HEP and EEP have the same rule with IP and EA. From these results, it is obvious that the introduction of electro-withdrawing groups allows the modulation of the electron affinity. This should be useful to enhance the electron transport from cathode in light-emitting diodes.

3.5.3. Charge transport

According to the Marcus/Hush model [27–29], the charge (hole or electron) transfer rate k can be expressed by the following formula:

$$K_{ET} = \frac{4\pi^2}{h}\frac{1}{\sqrt{4\pi\lambda K_B T}}t^2 \exp\left(-\frac{\lambda}{4K_B T}\right) \quad (1)$$

where t is the transfer integral, λ is the reorganization energy, T is the temperature, h and KB are the Plank and Boltzmann constants. Eq. (1) indicates that the rate of electron transfer depends on two main parameters: the reorganization energy (λ) and transfer integral (t). High transfer rate requires small values for λ and large values for t. Berlin concluded the reorganization energy could be an important factor that governs the mobility of charge carriers [30]. In this study, we draw our attention on the reorganization energy. The computational methods can be found in the literature [31].

The internal reorganization energies for hole and electron transfer are calculated by B3LYP/6-31G method. The reorganization energies for hole λ(h) and electron λ(e) of each compound are listed in Table 6. As observed in Table 6, the values of λ(h) for nine compounds are almost smaller than that of TPD, which is a typical hole transport material, is known to be 0.29 eV [31]. It is well known that the smaller the value of λ(h) is, the higher the hole transfer rate is. The value of λ(e) for OXD-X, OXD-A3, OXD-A7, OXD-TFM and OXD-C are almost smaller than that of Alq_3 which is a typical electron transport material and the value is 0.28 eV [32]. In addition, the λ(e) values for those compounds are smaller than the λ(h) values, which suggests that the electron transfer rate is better than the hole transfer rate, but different trend for OXD-N, OXD-N-1, OXD-N-2 and OXD-N-3. While the differences between λ(e) and λ(h) for OXD-X, OXD-A3, OXD-A7, OXD-TFM and OXD-C are much smaller than that of OXD-N, OXD-N-1, OXD-N-2 and OXD-N-3, which can greatly improve the charge transfer balance of former derivatives, thus further enhancing the device performance of OLEDs.

4. Conclusion

The results of the optimized structures indicate that the trans-conformation is more stable than the cis-one. The meta-substitution in the phenyl ring of OXD compounds generated less steric effect than that of ortho-substitutions. The frontier molecular orbitals analysis shows that the introduction of electron-withdrawing groups (–CN, $-CF_3$, $-NO_2$) results in the decrease of the energy levels of the FMOs. In addition, the $-NO_2$ substituted derivatives are more helpful for the electron injection than other derivatives. Furthermore, introducing fluorine in OXD-N is benefit for improving the electron-accepting abilities of OXD-N. Comparing with electron-donation groups, the absorption and emission spectra show that introducing electron-withdrawing groups mainly leads to the red shift of the absorption wavelengths, and blue shift of the emission wavelengths. In addition, the absorption and emission spectra of OXD-N can be further modulated through adjusting the position or the quantity of fluorine. The values of both λ(h) and λ(e) are smaller than typical hole and electron transport materials for OXD-X, OXD-A3, OXD-A7, OXD-TFM and OXD-C. Moreover, the charge transport ability for the electron and hole is nearly balanced, so, those compounds could be used as efficient and balanced carrier transport materials. As to OXD-N, OXD-N-1, OXD-N-2 and OXD-N-3, the λ(h) values for those compounds are smaller than the λ(e) values, which suggests that the hole transfer rate is better than the electron transfer rate.

Acknowledgments

This work is supported by the Training Fund of NENU'S Scientific Innovation Project (NENU-STC07016). We are greatly thankful for the referees' helpful comments.

References

[1] C.W. Tang, S.A. Van Slyke, Organic electroluminescent diodes, Appl. Phys. Lett. 51 (1987) 913–915.
[2] J.H. Lee, M.H. Wu, C.C. Chao, H.L. Chen, M.K. Leung, High efficiency and long lifetime OLED based on a metal-doped electron transport layer, Chem. Phys. Lett. 416 (2005) 234–237.
[3] C.A. Thomas, K. Zong, K.A. Abboud, P.J. Steel, J.R. Reynolds, Donor-mediated band gap reduction in a homologous series of conjugated polymers, J. Am. Chem. Soc. 126 (2004) 16440–16450.
[4] W.L. Yu, H. Meng, J. Pei, W. Huang, Y.F. Li, A.J. Heeger, Synthesis and characterization of a new *p–n* diblock light-emitting copolymer, Macromolecules 31 (1998) 4838–4844.
[5] J. Jacob, S. Sax, T. Piok, E.J.W. List, A.C. Grimsdale, K. Müllen, Ladder-type pentaphenylenes and their polymers: efficient blue-light emitters and electron-accepting materials via a common intermediate, J. Am. Chem. Soc. 126 (2004) 6987–6995.
[6] S. Oyston, C.S. Wang, G. Hughes, A.S. Batsanov, I.F. Perepichka, M.R. Bryce, J.H. Ahn, C. Pearson, M.C. Petty, New 2,5-diaryl-1,3,4-oxadiazole–fluorene hybrids as electron transporting materials for blended-layer organic light emitting diodes, J. Mater. Chem. 15 (2005) 194–203.
[7] M. Kawamoto, H. Mochizuki, T. Ikeda, H. Iino, J.I. Hanna, Charge carrier transport properties in polymer liquid crystals containing oxadiazole and amine moieties in the same side chain, J. Phys. Chem. B 109 (2005) 9226–9230.
[8] M. Kawamoto, H. Mochizuki, A. Shishido, O. Tsutsumi, T. Ikeda, B. Lee, Y. Shirota, Side-chain polymer liquid crystals containing oxadiazole and amine moieties with carrier-transporting abilities for single-layer light-emitting diodes, J. Phys. Chem. B 107 (2003) 4887–4893.
[9] F.I. Wua, C.F. Shua, C.H. Chienb, Y.T. Taob, Fluorene-based oxadiazoles: thermally stable electron-transporting materials for light-emitting devices, Synth. Met. 148 (2005) 133–139.
[10] S.H. Jin, M.Y. Kim, J.Y. Kim, K. Lee, Y.S. Gal, High-efficiency poly(*p*-phenylenevinylene)-based copolymers containing an oxadiazole pendant group for light-emitting diodes, J. Am. Chem. Soc. 126 (2004) 2474–2480.
[11] C.S. Wang, G.Y. Jung, Y.L. Hua, C. Pearson, M.R. Bryce, M.C. Petty, A.S. Batsanov, A.E. Goeta, J.A.K. Howard, An efficient pyridine- and oxadiazole-containing hole-blocking material for organic light-emitting diodes: synthesis, crystal structure, and device performance, Chem. Mater. 13 (2001) 1167–1173.
[12] L. Yang, Y. Liao, J.K. Feng, A.M. Ren, Theoretical studies of the modulation of polymer electronic and optical properties through the introduction of the electron-donating 3,4-ethylenedioxythiophene or electron-accepting pyridine and 1,3,4-oxadiazole moieties, J. Phys. Chem. A 109 (2005) 7764–7774.
[13] C. Risko, E. Zojer, P. Brocorens, S.R. Marder, J.L. Brédas, Bis-aryl substituted dioxaborines as electron-transport materials: a comparative density functional theory investigation with oxadiazoles and siloles, Chem. Phys. 313 (2005) 151–157.
[14] P. Zhang, B.H. Xia, Q.X. Zhang, B. Yang, M. Li, G. Zhang, W.J. Tian, New 1,3,4-oxadiazole containing materials with the effective leading substituents: the electrochemical properties, optical absorptions, and the electronic structures, Synth. Met. 156 (2006) 705–713.
[15] M.R. Pintoa, B. Hua, F.E. Karasza, L. Akcelrud, Emitting polymers containing cyano groups. Synthesis and photophysical properties of a fully conjugated polymer obtained by Wittig reaction, Polymer 41 (2000) 8095–8102.
[16] Y.H. Lee, Y.S. Kim, Theoretical study of Ir(III) complexes with cyclometalated alkenylquinoline ligands, Curr. Appl. Phys. 7 (2007) 504–508.
[17] J.H. Pan, H.L. Chiu, L. Chen, B.C. Wang, Theoretical investigations of triphenylamine derivatives as hole transporting materials in OLEDs: correlation of the Hammett parameter of the substituent to ionization potential, and reorganization energy level, Comput, Mater. Sci. 38 (2006) 105–112.
[18] M. Sugimoto, M. Anzai, K. Sakanoue, S. Sakaki, Modulating fluorescence of 8-quinolinolato compounds by functional groups: a theoretical study, Appl. Phys. Lett. 79 (2001) 2348–2350.
[19] Y.T. Tao, E. Balasubramaniam, Organic light-emitting diodes based on variously substituted pyrazoloquinolines as emitting material, Chem. Mater. 13 (2001) 1207–1212.
[20] G.C. Yang, T. Su, S.Q. Shi, Z.M. Su, H.Y. Zhang, Y. Wang, Theoretical study on photophysical properties of phenolpyridyl boron complexes, J. Phys. Chem. A 111 (2007) 2739–2744.
[21] M.J. Frisch, et al., Gaussian 03, Revision C.02, Gaussian Inc., Pittsburgh, PA, 2003.
[22] A.D. Becke, Density-functional exchange-energy approximation with correct asymptotic behavior, Phys. Rev. A 38 (1988) 3098–3100.
[23] A.D. Becke, A new mixing of Hartree–Fock and local density-functional theories, J. Chem. Phys. 98 (1993) 1372–1377.
[24] C. Lee, W. Yang, R.C. Parr, Development of the Colle-Salvetti correlation-energy formula into a functional of the electron density, Phys. Rev. B 37 (1998) 785–789.
[25] M.K. Casida, C. Jamorski, K.C. Cadida, D.R. Salahub, Molecular excitation energies to high-lying bound states from time-dependent density-functional response theory: characterization and correction of the time-dependent local density approximation ionization threshold, J. Chem. Phys. 108 (1998) 4439–4449.
[26] N.G. Park, G.C. Choi, Y.H. Lee, Y.S. Kim, Theoretical studies on the ground and excited states of blue phosphorescent cyclometalated Ir(III) complexes having ancillary ligand, Curr. Appl. Phys. 6 (2006) 620–626.
[27] R.A. Hush, Adiabatic rate processes at electrodes. I. Energy–charge relationships, J. Chem. Phys. 28 (1958) 962–972.
[28] R.A. Marcus, On the theory of oxidation–reduction reactions involving electron transfer. I, J. Chem. Phys. 24 (1956) 966–978.
[29] R.A. Marcus, Electron transfer reactions in chemistry. Theory and experiment, Rev. Mod. Phys. 65 (1993) 599–610.
[30] Y.A. Berlin, G.R. Hutchison, P. Rempala, M.A. Ratner, J. Michl, Charge hopping in molecular wires as a sequence of electron-transfer reactions, J. Phys. Chem. A 107 (2003) 3970–3980.
[31] M. Malagoli, J.L. Brédas, Density functional theory study of the geometric structure and energetics of triphenylamine-based hole-transporting molecules, Chem. Phys. Lett. 327 (2000) 13–17.
[32] B.C. Lin, C.P. Cheng, Z.Q. You, C.P. Hsu, Charge transport properties of tris(8-hydroxyquinolinato)aluminum(III): why it is an electron transporter, J. Am. Chem. Soc. 127 (2005) 66–67.